Removing arsenic from water with an original and modified natural manganese oxide ore: Batch kinetic and equilibrium adsorption studies

Thi Thuc Quyen Nguyen, Paripurnanda Loganathan, Tien Vinh Nguyen*, Saravanamuthu Vigneswaran

Faculty of Engineering and IT, University of Technology Sydney (UTS), Sydney, Australia

* Corresponding author: Tien Vinh Nguyen, Email: Tien.Nguyen@uts.edu.au; Tel: 61-2-95142620; Fax: 61-2-95147803

Abstract:

Arsenic contamination of drinking water is a serious water quality problem in many parts of the world. In this study, a low-cost manganese oxide ore from Vietnam (VMO) was firstly evaluated for its performance in arsenate (As(V)) removal from water. This material contains both Mn (25.6%) and Fe (16.1%) mainly in the form of cryptomelane and goethite minerals. At the initial As(V) concentration of 0.5 mg/L, the adsorption capacity of original VMO determined using the Langmuir model, was 0.11 mg/g. The modified VMOs produced by coating VMO with iron oxide (Fe^a-VMO) and zirconium oxide (Zr^a-VMO) at 110 ^{0}C and 550 ^{0}C achieved the highest As(V) adsorption capacity when compared to three other methods of VMO modifications. Langmuir maximum adsorption capacities of Fe^a-VMO and Zr^a-VMO at pH 7.0 were 2.19 mg/g and 1.94 mg/g, respectively, nearly twenty times higher than that of the original VMO. Batch equilibrium adsorption data fitted well to the Langmuir, Freundlich and Temkin models and batch kinetics adsorption data to pseudo-first order, pseudo-second order and Elovich models. The increase of pH progressively from 3 to 10 reduced As(V) adsorption with a maximum reduction of 50-60% at pH 10 for both original and modified VMOs. The co-existing oxyanions considerably weakened the As(V) removal efficiency because they competed with As(V) anions. The competition order was $PO_4^{3-} > SiO_3^{2-} > CO_3^{2-} > SO_4^{2-}$. The characteristics of the original and modified VMOs evaluated using SEM, FTIR, XRD, XRF, surface area, and zeta potential explained the As(V) adsorption behaviour.

Keywords: Arsenic; manganese oxide ore; iron oxide and zirconium oxide modification; adsorption; water treatment

1. Introduction

Inorganic arsenic (As) is one of the most serious and challenging pollutants that must be removed from water sources because it is highly toxic in drinking water (Sogaard 2014). Arsenic contamination of water is prevalent in several countries because of natural geological processes and human activities such as mining, chemical industries, and groundwater exploitation (Järup 2003). The range of As concentration in water varies widely from below 0.001 mg/L up to 1.0 mg/L; in some places, it can even reach 3.0 mg/L or higher (Amini et al. 2008; Berg et al. 2001). These concentrations are much higher than the WHO recommended As concentration in drinking water of 0.01 mg/L. In some well-known contaminated regions in Asia, such as Bangladesh, India, Nepal and Vietnam, the common As concentration in the affected areas is 0.2 - 0.5 mg/L (Berg et al. 2007; Berg et al. 2001; Buschmann et al. 2007; Chakraborti et al. 2002; Polya et al. 2005; Smedley and Kinniburgh 2002). The most common As species in groundwater are arsenate As(V) and arsenite As(III).

Several studies have demonstrated that various techniques can remove As, for example, coagulation, adsorption, ion exchange, and membrane separation (Maiti et al. 2010). Choosing the best appropriate As removal technology is based on many factors: water characteristics, treatment cost, treatment target, treatment efficiency, application conditions, etc. Removing As through adsorption technology has many advantages such as low-cost, simple implementation, high efficiency at a wide range of concentrations, and minimum waste production. It is also suitable for application in decentralized systems in affected areas, especially in developing countries where the As problem mostly occurs.

A wide range of materials, both natural and synthetic media, have been used as adsorbents for As removal. Some commercial and synthetic media such as activated carbon, activated alumina and Zr resin have produced a very high As removal capacity, i.e. over 10 mg/g (Mohan and Pittman Jr 2007). Several natural materials or waste industrial/agricultural products (including sand, natural clay, kaolinite clay, bentonite, laterites, manganese ore, iron ore, dry plants, red mud, fly ash, etc.) have emerged as low-cost As removal options (Ahmed 2001; Chakravarty et al. 2002; Chiban et al. 2012). Unlike commercial products, some natural materials cannot reach As adsorption capacity higher than 1 mg/g. For example, the capacity of red mud is 0.514 mg/g, and kaolinite clay is below 0.23 mg/g (Altundoğan et al. 2002; Mohan and Pittman Jr 2007). In some cases, they could not even meet the As permissible limit for practical application (Kabir and Chowdhury 2017). However, when compared to the most popular and efficient As adsorbent, such as activated carbon which has a high price and regeneration cost, the natural materials' advantages are cost-effectiveness, mechanical stability and local availability in many As affected areas (Chiban et al. 2012). This has encouraged researchers to promote the use of low-cost locally available natural adsorbing materials.

Natural manganese oxide ore is a popular low-cost material that has been used to remove both As(III) and As(V) (Ahmed 2001; Chakravarty et al. 2002). However, the adsorption capacity of this ore is generally low (Chakravarty et al. 2002), and for this reason, it is difficult to use it widely and compete with other adsorbents having higher adsorption capacity. Chemical modifications can significantly improve the adsorption capacity of adsorbent media (Asere et al. (2019). For example, modification of clinoptilolite-Ca zeolite using manganese dioxide doubled the adsorption capacity of the unmodified zeolite (Camacho et al. 2011). The modification of biochar using magnetic gelatin also increased As adsorption capacity by about three times (Zhou et al. 2017). Pokhrel and Viraraghavan (2008) reported that iron oxide-coated biomass (IOCB) improved the efficiency significantly in removing As compared to uncoated materials.

Among the many chemicals used as modified agents, water-insoluble metal oxides are the best choice (Khan et al. 2013). Coating low-cost materials with iron (Fe) oxide and zirconium (Zr) oxide is considered an efficient method because of the high affinity of Fe and Zr towards As adsorption (Khan et al. 2013; Mohan and Pittman Jr 2007; Pokhrel and Viraraghavan 2008).

In this study, a low-cost manganese oxide ore from Vietnam (VMO) with and without modification was tested as an adsorbent for As(V) removal from aqueous solution in batch kinetics and equilibrium adsorption studies. The modification was carried out by coating VMO with Fe oxide and Zr oxide under four different coating conditions and the modification that produced the highest adsorption capacity was chosen for detailed studies. These included testing the effects of pH and coexisting anions (PO_4^{3-}, SiO_3^{2-}, SO_4^{2-}, CO_3^{2-}) on adsorption as well as determining the mechanism of adsorption.

2. Material and Methods

2.1 Feed solution

In this study, 1 L synthetic stock solution was prepared by dissolving sodium arsenate ($Na_2HAsO_4 \cdot 7H_2O$) in Milli-Q water to obtain a concentration of 10 mg As(V)/L. This stock solution was then diluted to desired concentrations for use in the experiments. The solution's ionic strength was maintained at 1×10^{-3} M $NaNO_3$ and the solution pH was adjusted to 7.0 ± 0.2 by adding diluted nitric acid (0.1 M HNO_3) and sodium hydroxide (0.1 M NaOH).

2.2 Original adsorbent

A commercial Vietnamese manganese oxide (VMO) (particle size 0.1-3.0 mm), which is a mineral waste originating from the Tuyen Quang mine, and supplied by Phuong Nam Import-Export Trading and Service Joint Stock Company, Ha Noi, Vietnam, was used as an adsorbent for As. It is a low-cost material and employed locally as an adsorbent in water treatment systems. The VMO was ground and sieved into three different sizes - 0.3 - 0.6 mm, 0.6 - 1.0 mm and 1.0 - 2.0 mm - to study the effect of particle size on the VMO adsorption performance towards As. The sieved materials were washed by deionized distilled water and diluted nitric acid (0.1 M HNO_3) to remove any dirt and soluble compounds adhering to its surface. Then it was dried at 100 ^{0}C for 24 h to remove excess water and moisture before being stored in tightly closed plastic bags.

2.3 Modified adsorbents

Modified VMOs were produced from VMO with a particle size of 0.3-0.6 mm using four coating methods. Both Fe and Zr were used as coating agents. Below are the details of the modification processes:

- *Fe^a-VMO*: 200 g of VMO was poured into a mixture of 80 mL 2 M ferric nitrate nonahydrate ($Fe(NO_3)_3 \cdot 9H_2O$) and 1 mL 10 M NaOH and shaken manually for 5 min. The mixture was heated at 110 ^{0}C for 4 h and then at 550 ^{0}C for 3 h for the first time. After cooling and washing the mixture, 100 g of this material was poured into a similar mixture as before and heated again at 110 ^{0}C for 20 h. This modification procedure is an adaptation of the method used by Thirunavukkarasu et al. (2003) for preparing iron oxide coated sand (IOCS-2).

- *Fe^b-VMO*: VMO was modified again by impregnation of iron. 10 g VMO was mixed with 1 L ferric chloride hexahydrate $FeCl_3.6H_2O$ (2.0 g Fe^{3+}/L) and the mixture was shaken for 1 h at 120 rpm. Then, the pH of the mixed solution was adjusted to 8.0 by adding 1 M NaOH. After 3 h of continuous shaking, the shaking speed was reduced to 30 rpm and the suspension was intermittently mixed for 24 h. The material was then rinsed by Milli-Q water to remove unreacted Fe and dried at 45 ^{0}C for 24 h (Kalaruban et al. 2016).

- *Fe^c-VMO*: This material was prepared by adding 10 g VMO to 150 mL solution of 0.1 M ferrous chloride tetrahydrate ($FeCl_2.4H_2O$) at pH 4.2 - 4.5 and agitated at 120 rpm for 24 h at room temperature (25 ± 1 °C). This was followed by washing it with 200 mL Milli-Q water three times and drying at 80 °C for 4 h (Gu et al. 2005).

- *Fe^d-VMO*: The preparation procedure was similar to that of Fe^c-VMO. However, 20 mL sodium hypochlorite (13% NaClO) was added four times to the 150 mL solution during the shaking phase, each at intervals of 6 h. In this process, pH was maintained at 4.5 - 5.0 (Gu et al. 2005).

Similarly, Zr^a, Zr^b, Zr^c, Zr^d were produced by mixing zirconyl chloride octahydrate ($ZrOCl_2.8H_2O$) instead of the iron salts with VMO according to the above methods.

2.4 As(V) adsorption capacity of modified and unmodified VMOs with different particle sizes

Unmodified VMO of doses 1 - 5 g/L with particle sizes of 0.3 - 0.6 mm, 0.6 - 1.0 mm and 1.0 - 2.0 mm were added into 250 mL flasks containing 100 mL As(V) solution of 0.1 mg/L concentration. These flasks were shaken at 120 rpm for 24 h. The supernatant solution was filtered using 0.45 µm filters and filtered samples were analyzed for As using an ICP-MS instrument (Agilent Technologies 7900 ICP-MS). Similar experiments were also conducted with the eight types of modified VMO of the same particle size of 0.3-0.6 mm. In all studies, the initial pH and ionic strength were 7.0 ± 0.2 and 1×10^{-3} M NaNO$_3$, respectively.

The results (presented in more detail in Section 3.1) demonstrated that VMO of particle size 0.3-0.6 mm and Fe^a-VMO and Zr^a-VMO had the highest As(V) adsorption capacity. Consequently, they were chosen for the subsequent studies and characterisation.

2.5 Equilibrium and kinetic adsorption of As(V) on VMO, Fe^a-VMO and Zr^a-VMO

All batch experiments were conducted on VMO, Fe^a-VMO and Zr^a-VMO (particle size 0.3-0.6 mm) at room temperature of 25 ± 1 ^{0}C and natural pH of 7.0 ± 0.2 (excluding experiments on pH impact). The ionic strength was kept at 1×10^{-3} M NaNO$_3$ for all feed solutions.

The equilibrium adsorption experiments were conducted by adding different adsorbent dosages, i.e. 2.0 - 14 g/L of VMO and 0.1 - 2.0 g/L of modified VMO, into a set of flasks containing 100 mL As(V) solution of 0.5 mg/L. The flasks were agitated on a shaker at 120 rpm for 24 h. The supernatant solutions were filtered using 0.45 µm filters and As in filtered samples was analysed.

The amount of As(V) adsorption at equilibrium was calculated using Equation 1 (Nur et al. 2014):

$$q_e = \frac{(C_0 - C_e) \cdot V}{M} \quad (mg/g) \qquad [1]$$

where C_0 is initial concentration of As(V) (mg/L), C_e is equilibrium concentration of As(V) (mg/L), V is volume of solution (L) and M is mass of adsorbent (g)

Adsorption efficiency was calculated using equation 2 as follows:

$$E(\%) = \frac{(C_0 - C_e)}{C_0} \times 100 \qquad [2]$$

The adsorption kinetics experiment was conducted by adding predetermined amounts of VMO (2 g/L) and modified VMO (0.1 mg/L) into a set of flasks containing 100 mL solution of 0.5 mg/L As(V). The flasks were then agitated at 120 rpm, and samples were taken at different time intervals, ranging from 5 min to 24 h.

The adsorption equilibrium and kinetic data was modelled using common adsorption models (Table 1).

Table 1. The equilibrium (Dada et al. 2012) and kinetic (Qiu et al. 2009; Wu et al. 2009) adsorption models

Experiment	Model	Equation*	Parameter
Equilibrium	Langmuir	$q_e = \dfrac{q_m . k_L . C_e}{(1 + k_L . C_e)}$ $R_L = \dfrac{1}{1 + (1 + k_L . C_0)}$	q_m, k_L, R_L
	Freundlich	$q_e = k_f . C_e^{1/n}$	k_f, n
	Temkin	$q_e = \dfrac{RT}{b_T} . \ln(A_T . C_e)$ $B = \dfrac{RT}{b_T}$	A_T, B, b_T
Kinetics	Pseudo-first order	$\dfrac{dq_t}{dt} = k_1(q_e - q_t)$	k_1, q_e
	Pseudo-second order	$\dfrac{dq_t}{dt} = k_2(q_e - q_t)^2$	k_2, q_e
	Elovich	$\dfrac{dq_t}{dt} = \alpha e^{-\beta q_t}$	α, β

* q_e is the amount of As adsorbed per unit mass of adsorbent (mg/g), q_m is the maximum amount of the As adsorbed per unit mass of the adsorbent (mg/g), k_L is Langmuir isotherm constant (L/mg), C_e is the As concentration in solution at equilibrium (mg/L), C_0 is the initial As concentration (mg/L), R_L is equilibrium parameter; k_f and n are the Freundlich constants; A_T is Temkin isotherm equilibrium binding constant (L/g), b_T is Temkin isotherm constant (kJ/mol), R is universal gas constant (8.314 J/mol/K), T is room temperature at 298K, and B is constant related to heat of sorption (J/mol). * q_e is the amount of As adsorbed at equilibrium (mg/g), q_t is the amount of As adsorbed at time t (mg/g), k_1 is the rate constant of pseudo-first order adsorption (L/h), k_2 is the rate constant of pseudo-second order (g/mg.h), α is the initial adsorption rate (mg/g.min), β is related to the extent of surface coverage and activation energy for chemisorption (g/mg).

2.6 pH influence on As(V) adsorption

Experiments on pH influence on As(V) adsorption were conducted at a pH range from 3.0 to 10.0. Here, pH of As(V) solution was adjusted using 0.1 M HNO_3 and 0.1 M NaOH solutions after the required amounts of modified VMO (0.3 g/L) and unmodified VMO (3 g/L) were added to a set of glass flasks containing 100 mL of 0.5 mg As(V)/L. The experimental procedure was similar to the previous equilibrium adsorption experiment.

2.7 Coexisting anions' influence on As(V) adsorption

A study on the influence of coexisting anions on As(V) adsorption was carried out utilising four typical anions, i.e. phosphate (PO_4^{3-}), sulphate (SO_4^{2-}), silicate (SiO_3^{2-}) and bicarbonate (CO_3^{2-}). In this experiment, Na^+ salts of different anions of concentration from 0.1 to 20 mg/L were added separately into 100 mL solutions containing 0.5 mg As(V)/L. Predetermined amounts of 0.1 g modified VMO and 1 g unmodified VMO were added to the above solutions. The experimental procedure was similar to that of the previous equilibrium adsorption experiments.

2.8 Adsorbent characterisation

Characteristics of unmodified and modified VMOs were determined by: X-ray diffraction (XRD, Bruker D2 Phaser instrument); Scanning electron microscopy (SEM; Quanta-650 instrument); Fourier transform infrared (FTIR, Nicolet iS5 FT-IR Spectrometer); X-ray fluorescence (XRF, Olympus Vanta M series); and Brunauer-Emmett-Teller (BET) nitrogen adsorption.

Zeta potential measurement was done to determine the surface charge characteristics of materials before and after As(V) adsorption. Here, the zeta potentials of suspensions prepared by adding 0.1 g of fine material (<0.75 µm) in 100 mL Milli-Q water at different pHs were measured using a Zetasizer nano instrument, Nano ZS Zen 3600.

3. Results and discussion

3.1 Characteristics of adsorbents

Elemental compositions of unmodified and modified VMO as determined by XRF are shown in Table 2. The unmodified VMO had high percentages of Mn and Fe and a moderate percentage of Si, but no Zr. The composition was found to be strongly dependent on the coating conditions. The modified materials, Fe[a]-VMO and Zr[a]-VMO produced by the first modification process (mixing original VMO with ferric nitrate and sodium hydroxide and heating at high temperature) had the highest percentage of Fe and Zr after modification (21.9% and 9.8%, respectively). Coating metals on VMO increased the percentages of these metals in Fe[a]-VMO and Zr[a]-VMO by approximately 6 and 10%, respectively. Additionally, after As(V) adsorption, the percentages of Fe and Zr did not decrease, indicating a strong coating of these metals. Therefore, there is no risk of heavy metals leaching from the adsorbents and creating secondary pollution in the treated water.

Table 2. Metals composition of original and modified VMO determined by XRF

| Adsorbent	Si (wt%)	Mn (wt%)	Fe (wt%)	Zr (wt%)	Al (wt%)
Before As adsorption					
VMO	13.0 ± 0.1	25.6 ± 0.2	**16.1 ± 0.0**	0	2.5 ± 0.1
Fe[a]-VMO	8.7 ± 0.1	20.9 ± 0.2	**21.9 ± 0.2**	0	2.0 ± 0.1
Fe[b]-VMO	15.2 ± 0.1	16.7 ± 0.1	**20.0 ± 0.1**	0	3.1 ± 0.1
Fe[c]-VMO	14.4 ± 0.1	19.9 ± 0.1	**19.0 ± 0.1**	0	2.9 ± 0.1
Fe[d]-VMO	14.3 ± 0.1	19.7 ± 0.1	**19.1 ± 0.1**	0	3.0 ± 0.1
Zr[a]-VMO	7.4 ± 0.1	22.5 ± 0.3	12.2 ± 0.2	**9.8 ± 0.1**	1.4 ± 0.1
Zr[b]-VMO	13.0 ± 0.1	21.6 ± 0.1	19.0 ± 0.1	**0.1 ± 0.1**	2.9 ± 0.1
Zr[c]-VMO	13.6 ± 0.1	23.4 ± 0.1	18.5 ± 0.1	**0.08 ± 0.1**	2.8 ± 0.1
Zr[d]-VMO	13.7 ± 0.1	19.9 ± 0.1	18.9 ± 0.1	**0.5 ± 0.1**	2.8 ± 0.1
After As adsorption					
VMO	13.1 ± 0.1	26.0 ± 0.2	**16.4 ± 0.0**	0	2.4 ± 0.1
Fe[a]-VMO	9.9 ± 0.1	25.0 ± 0.2	**23.1 ± 0.1**	0	2.2 ± 0.1
Zr[a]-VMO	7.6 ± 0.1	24.2 ± 0.2	13.6 ± 0.1	**10.2 ± 0.1**	1.3 ± 0.1

Fig. 1a, b, c, d, e, and f show the surface morphologies of original VMO and Fe[a]-VMO and Zr[a]-VMO, before and after As adsorption determined by SEM at a high magnification of 3200x, respectively. The relatively irregular and heterogeneous surface morphology of the three materials can be clearly seen in these figures. The images also indicated that both Fe[a]-VMO and Zr[a]-VMO possessed more porous layers/channels than the original VMO. No visible change in the surface morphologies of the materials were observed after As adsorption.
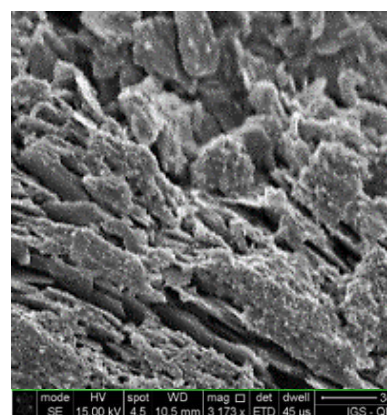
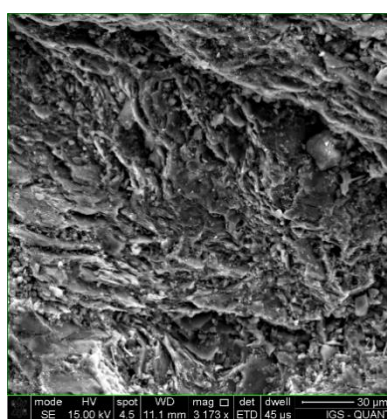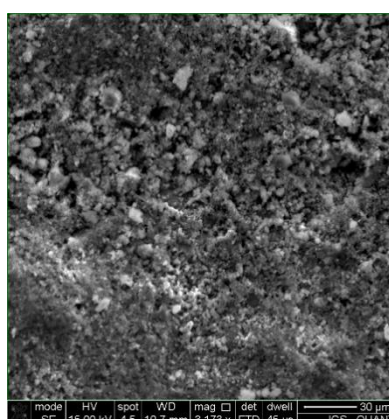**Before As adsorption**

(a) VMO
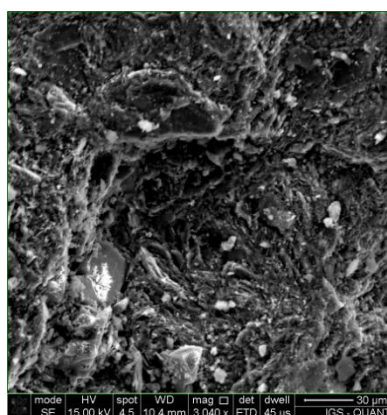
(b) Feᵃ-VMO
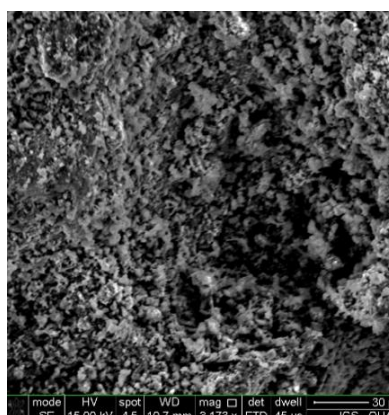
(c) Zrᵃ-VMO

After As adsorption

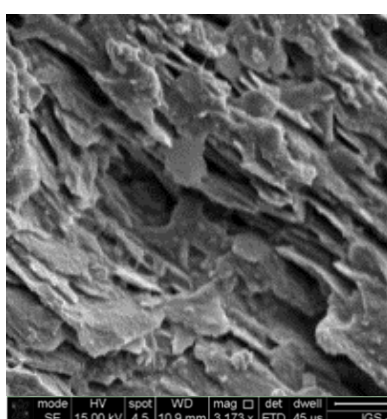(d) VMO + As

(e) Feᵃ-VMO+As

(f) Zrᵃ-VMO+As

Fig. 1. SEM images of VMO before, after coating and adsorption.

A material's adsorption ability strongly depends on its mineral components. According to the XRD diagram (Fig. 2), VMO consists of four main minerals, namely quartz, goethite, cryptomelane and muscovite. Quartz and muscovite contributed to the high content of silicon (13%) in VMO; goethite to the high content of Fe (16.1%); and cryptomelane to the high content of Mn (25.6%) (Table 2). Fe modification of VMO slightly changed the XRD pattern. This modification produced new peaks characteristics of hematite (an Fe oxide mineral). It also appears that the goethite peaks in the unmodified VMO were reduced in size. This indicates that some of the goethite might have got transformed into hematite at the high temperatures used in the modification procedure and/or the Fe coatings might have produced the hematite mineral. Zr coating of VMO also produced new XRD peaks which are characteristics of zirconia minerals such as zirconia/zirconolite. It could also be possible that the Fe and Zr added might have formed some amorphous (non-crystalline) compounds which cannot be identified by XRD. As adsorption did not change the XRD pattern probably either because of the small amounts of As concentration compared to other elements in the adsorbents or the As compounds formed were amorphous that cannot be detected by XRD. The hematite produced as a result of Fe and Zr coatings at high temperature and reduction in the peak heights of goethite is expected to increase the As(V) adsorption capacity of VMO. Mamindy-Pajany et al. (2011) reported that As(V) adsorption capacity of hematite is more than double that of goethite. The zirconia mineral produced by Zr coating of VMO is also expected to increase the As(V) adsorption capacity (Hang et al. 2011).
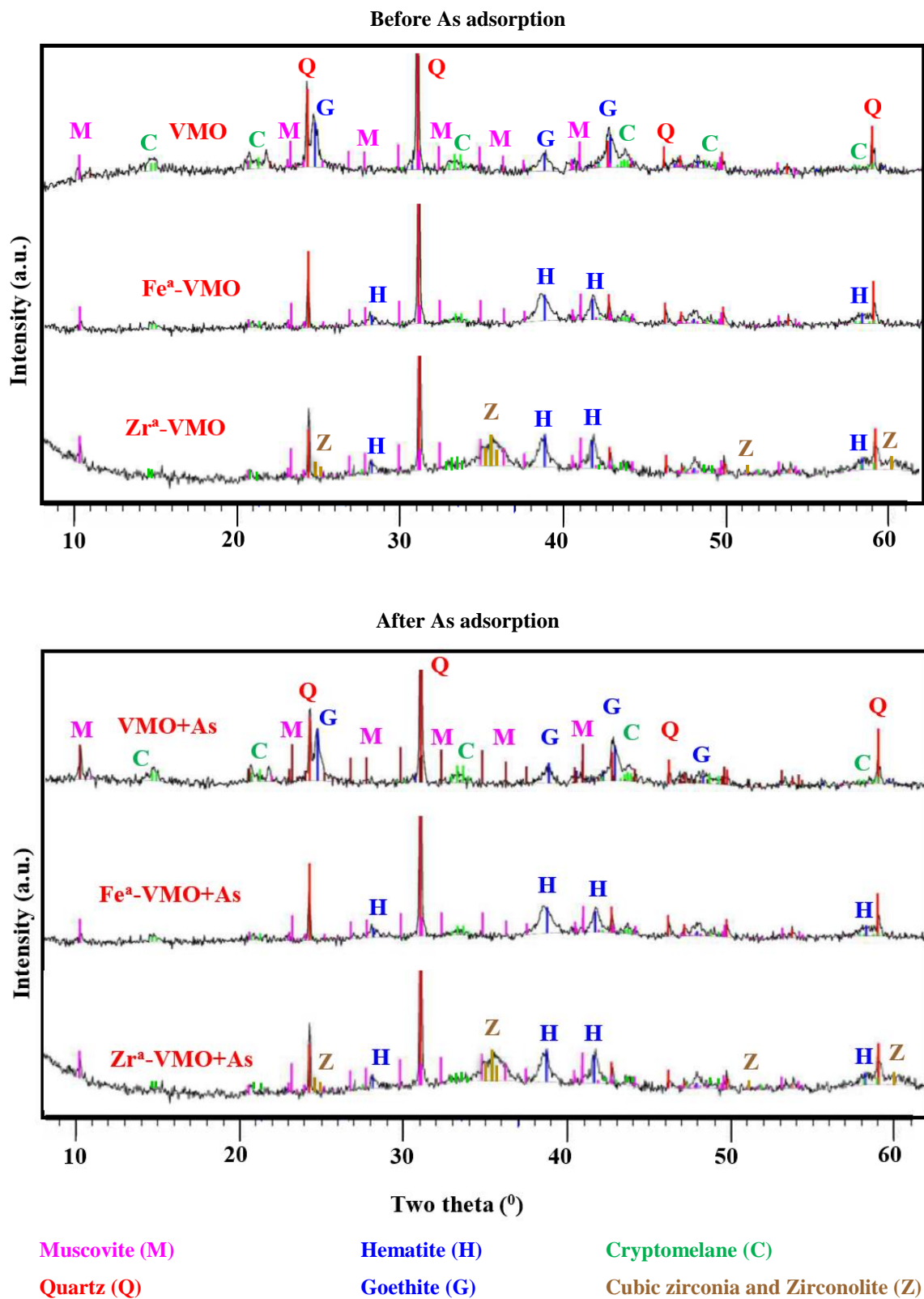
Fig. 2. XRD diagram of VMO and modified VMOs before and after As adsorption

BET surface areas of VMO and its modified forms were 27.1 and 37.1-37.5 m²/g, respectively (Table 3). These values are higher than those of many other natural As adsorbents such as gibbsite, goethite, kaolinite, and iron oxide coated sand (Mohan and Pittman Jr 2007). However, their BET surface area values are lower than those

of the popular commercial adsorbents such as activated carbon and activated alumina (Mohan and Pittman Jr 2007). Table 3 also shows that the surface area of VMO increased significantly after modification. This may have been triggered by the creation of porous forms of Fe and Zr precipitated particles. However, the BET surface area and pore volume of both original and modified VMO decreased after adsorption (Table 3). It could be because of the adsorption of As(V)/or formation of As(V) compounds on the surface of the adsorbent and filling-up of some of the pores inside the adsorbent.

Table 3. BET surface area and pore volume of adsorbents

Adsorbent	Before As(V) adsorption		After As(V) adsorption	
	BET (m^2/g)	Pore volume (cm^3/g)	BET (m^2/g)	Pore volume (cm^3/g)
VMO	27.1	0.0022	17.3	0.0012
Fe[a]-VMO	37.5	0.0017	24.4	0.0004
Zr[a]-VMO	37.1	0.0022	26.6	0.0006

FTIR diagrams (Fig. 3) depict the presence of some chemical bonds on the adsorbents before and after As(V) adsorption process. Evaluation of the differences in the peak intensity, peak shifting and peak appearance (or disappearance) indicates the types of interaction between surface chemical groups and absorbed As(V).

Generally, the FTIR shapes of the three adsorbents are not too different. After coating, some new peaks appeared that represent new bonds between Fe or Zr with available functional groups. Fig. 3a shows that a vibrational spectrum exhibited broad O-H stretching peaks between 3700 and 3300 cm^{-1}, and O-H bending at 1640 cm^{-1} (Myneni et al. 1998; Petit and Puskar 2018; Tomić et al. 2011). The peak of 1384 cm^{-1} could be ascribed to the vibration of C-H (Delva et al. 2013). The bands between 1100 and 900 cm^{-1} are normally assigned to Fe-OH bending, Al-OH bending and Si-O stretching vibration (Tomić et al. 2011; Zhang et al. 2009). The peaks at 794 cm^{-1} and nearby could be attributed to Fe-O (Jia et al. 2007; Tomić et al. 2011). Many peaks were also observed at 525, 524, 523 and 466, 454, 419 cm^{-1}. According to previous reports, these peaks could be assigned to the functional groups of metal such as Mn-O, Mn-O-M, Zr-O-Zr, Si-O-Al, and Si-O-Si (Markovski et al. 2014; Tomić et al. 2011).

Fig. 3b illustrates that all peaks of the adsorbents reduced evenly after adsorption. Moreover, it shows that no new group appears in the FTIR diagram. It means that As(V) only reacted with the available functional groups of adsorbents.
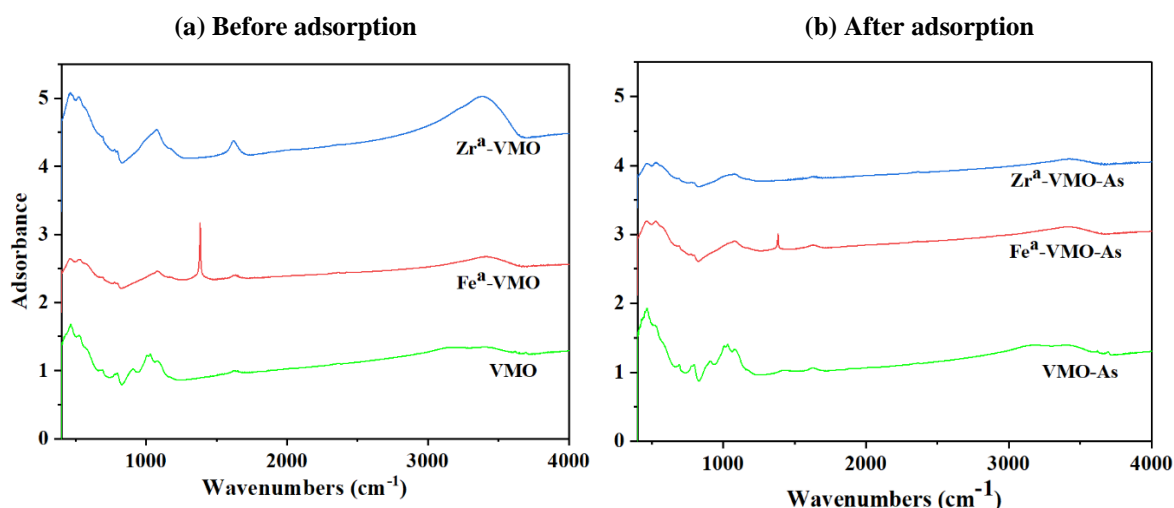
Fig. 3. FTIR diagram of original and modified VMO before and after As(V) adsorption

Zeta potential of original and modified VMOs at different pHs is presented in Fig. 4. The data shows that zeta potentials of Fe[a]-VMO and Zr[a]-VMO were more positive than unmodified VMO at all pHs (Fig. 4a). This means that the impregnation of Fe and Zr on VMO increased the surface positive charge of VMO. As(V) often exists in anionic forms, depending on pH in water (monovalent $H_2AsO_4^-$, divalent $HAsO_4^{2-}$ and trivalent AsO_4^{3-} within the pH range from approximately 3.0 to 6.0, 7.0 to 11, and 12 to 14, respectively) (Mondal et al. 2007). Therefore, the appearance of a more positive charge on modified VMO is favourable for As(V) removal from water through electrostatic adsorption forces.

The zero point of charges (ZPC, pH at which net surface charge is zero) of VMO, Fe[a]-VMO and Zr[a]-VMO were at pH 6.3, 7.1 and 7.5, respectively. At pH lower than ZPC, the zeta potentials were more positive and at pH higher than ZPC they were more negative (Loganathan et al. 2014; Oladoja and Helmreich 2014). During As(V) adsorption process, because As(V) exits in negatively charged forms, the original and modified VMO had a better tendency to adsorb As(V) at lower pH through electrostatic forces. In contrast, at higher pH, especially at basic conditions, the surface charges of original and modified VMO change from positive to negative. This leads to a reduction of As(V) adsorption capacity of these materials.

Fig. 4b shows that the negative zeta potentials decreased at all pHs and the zero point of charge reduced when the negatively charged As(V) adsorbed on all adsorbents. The decrease of zeta potential indicates that As species were adsorbed on the surface of the adsorbent by inner-sphere complexation as well (ligand exchange) (Kalaruban et al. 2016; Loganathan et al. 2014).
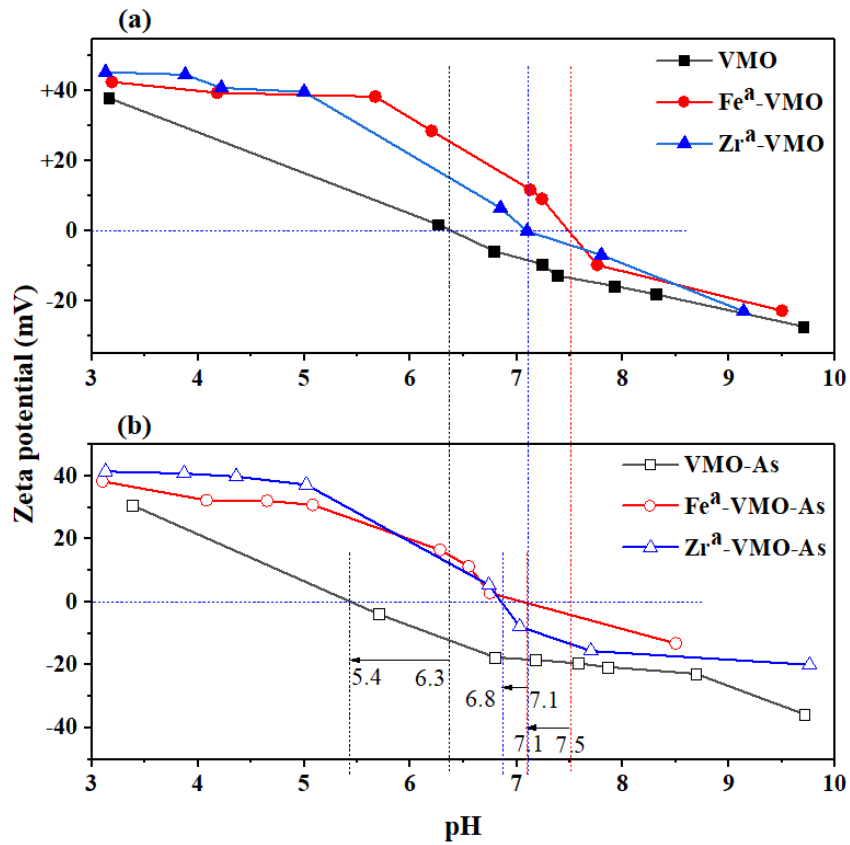
Fig. 4. Zeta potential of adsorbents (a) before and (b) after As(V) adsorption

3.2 Effect of particle size on As(V) adsorption

As(V) adsorption efficiency (E%) increased with adsorbent doses and reduction in particle size (Fig. 5). At the highest dosage of 5 g/L, the E% of particle size 1.0-2.0 mm was only 38% while that of smaller sizes of 0.3-0.6 mm and 0.6-1.0 mm reached up to 90% and 84%, respectively. With the original commercial size, which is a mix of all sizes, E% was approximately 52%. The particle size of 0.3-0.6 mm was chosen for experimentation in the subsequent studies because of its highest E%.
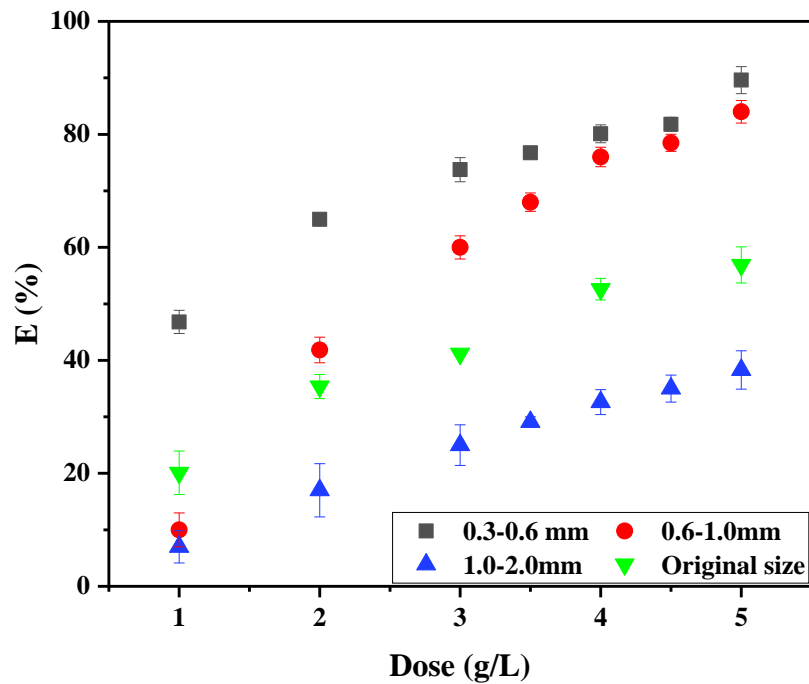
Fig. 5. Effect of particle size on As(V) removal efficiency

3.3 Effect of modification method on As(V) adsorption

Fig. 6 shows that the coating of Fe and Zr on VMO material has improved the material's capacity to remove As(V). However, the level of improvement strongly depended on the modification methods. The Fe^a-VMO and Zr^a-VMO had the highest improvement. At the dose of 1g, the As(V) removal efficiency of modified Fe^a-VMO and Zr^a-VMO was nearly five times higher than that of the unmodified VMO. The other three modification processes were less effective and only a slight improvement in As(V) removal was observed.
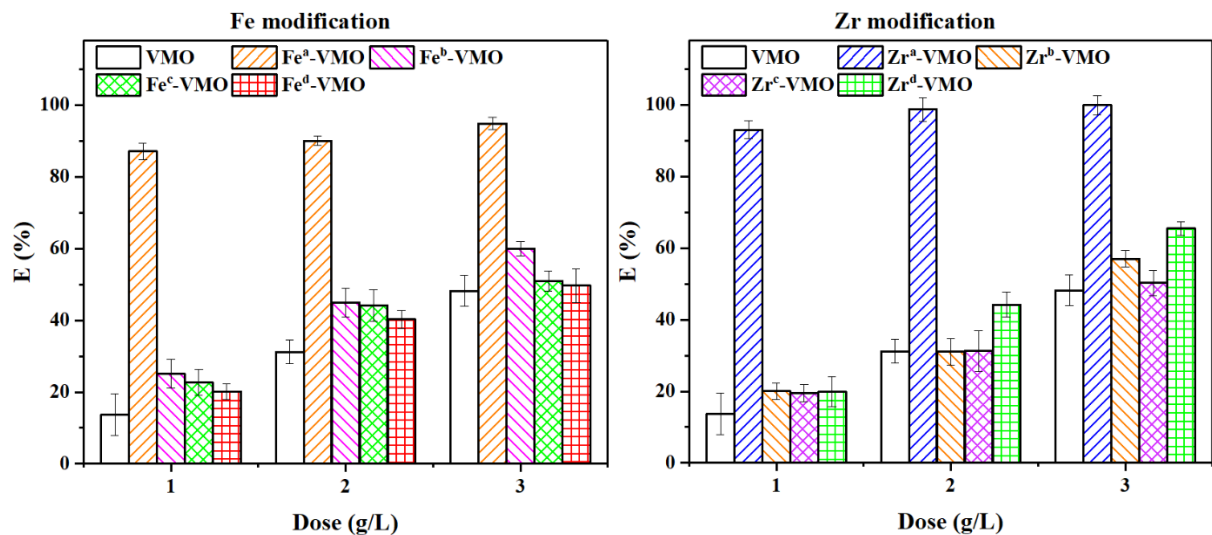

Fig. 6. Effect of different methods of VMO modification on As(V) removal efficiency

Temperature played an important role in the effectiveness of the modification processes. The Fe^a and Zr^a modification method applied to the production of Fe^a-VMO and Zr^a-VMO involved a light agitation followed by heating at high temperature of 110 ^{0}C and 550 ^{0}C. Here, the modification temperatures were higher than those

used in the other three methods (less than 80 ^0C). At extremely high temperature, the coating agents might have adhered strongly to the surface of the VMO. Solutions used to wash Fe[a]-VMO and Zr[a]-VMO after their preparation were colourless compared to those in other preparations, suggesting strong coatings at high temperature. The Fe and Zr contents of these modifications were also higher than those produced at lower temperatures (Table 2). Moreover, a high temperature would also have raised the surface area of the samples (Thirunavukkarasu et al. 2003). Based on these findings, Fe[a]-VMO, Zr[a]-VMO and unmodified VMO were used in the subsequent studies.

3.4 Equilibrium and kinetics adsorption studies

3.4.1 Equilibrium adsorption isotherms

The equilibrium adsorption experiments for the three adsorbents were conducted at pH 7.0 ± 0.2 with different adsorbent dosages. The Langmuir, Freundlich and Temkin models were employed to describe the data of the adsorption isotherms (Fig. 7). Table 4 shows that the experimental data fitted well to all three isotherm models with the Freundlich model having the best fit ($R^2 = 0.90 - 0.97$), followed by the Langmuir ($R^2 = 0.87 - 0.95$) and Temkin ($R^2 = 0.82 - 0.95$). Better fit to the Freundlich model is probably because of the heterogeneous adsorption sites on VMO and modified VMO such as the different adsorption sites on Mn and Fe minerals (Fig. 2) and Zr and Fe coatings. The Langmuir adsorption capacity of VMO increased considerably after modification. Adsorption capacities of Fe[a]-VMO and Zr[a]-VMO were 2.19 mg As/g and 1.94 mg As/L, respectively. These values are nearly twenty times higher than that of the original VMO (0.11 mg As/g) (Table 4). It indicates that the presence of Fe^{3+} and Zr^{4+} ions on the surface of VMO improved significantly the As(V) adsorption capacity of VMO. The improvement is due to the strong adsorption of the anionic arsenic species on Fe^{3+} and Zr^{4+} hydroxide/oxides on the surface of VMO (Loganathan et al. 2014; Sogaard 2014). The new minerals (hematite, zirconia/zirconolite and amorphous minerals) formed as a result of Fe and Zr coatings (Fig. 2) would have enhanced the adsorption capacities as discussed in Section 3.1.
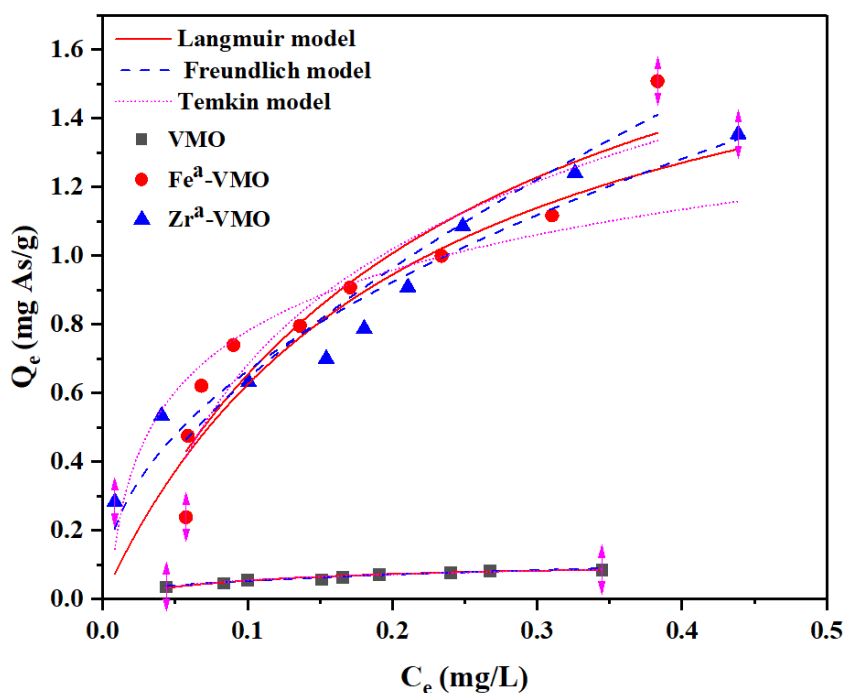

Fig. 7. Batch equilibrium adsorption models fit adsorption data for VMO and modified forms of VMO

The R_L value obtained from the Langmuir model fit indicates the nature of adsorption. Adsorption is considered unfavourable if $R_L > 1$, linear if $R_L = 1$, favourable if $0 < R_L < 1$ and irreversible if $R_L = 0$ (Dada et al. 2012). The calculated R_L data of VMO, Fe[a]-VMO, Zr[a]-VMO were 0.15, 0.24 and 0.23, respectively (Table 4). All these values are between 0 and 1 indicating that the adsorption process is favourable for both original and modified VMOs.

In contrast to the Langmuir model, the Freundlich model is used to depict the adsorption characteristics for the heterogeneous surface with multilayer adsorption (Dada et al. 2012). The calculated k_f parameter value from the Freundlich model decreased in the following order: Fe[a]-VMO (2.48) > Zr[a]-VMO (1.98) > VMO (0.14). This is in the same order of As(V) adsorption capacity calculated using the Langmuir model. Additionally, all values of $1/n$ are below 1 indicating that the adsorption of As(V) by these adsorbents is favourable confirming the findings from Langmuir R_L values.

Unlike the Langmuir and Freundlich models, the Temkin model is usually used for heterogeneous surface energy systems (Erhayem et al. 2015; Shahmohammadi-Kalalagh 2011). It contains a factor that explicitly takes into account of adsorbent- adsorbate interactions (Dada et al. 2012). According to the calculated data in Table 4, the B values related to heat of sorption are positive indicating that the sorption process is exothermic and the values are higher for modified VMOs (Puttamat and Pavarajarn 2016).

Table 4. Parameter values for batch equilibrium adsorption models

Model	Parameter	Adsorbent		
		VMO	Fe[a]-VMO	Zr[a]-VMO
Langmuir	q_m (mg As/g)	0.11	2.19	1.94
	k_L (L/mg)	8.93	4.24	4.75
	R_L	0.15	0.24	0.23
	R^2	0.95	0.89	0.87
Freundlich	k_f (mg/g) (L/mg)$^{1/n}$	0.14	2.48	1.98
	N	2.34	1.70	2.11
	R^2	0.97	0.90	0.95
Temkin	A_T (L/g)	84.27	40.63	211.75
	B (J/mol)	0.025	0.49	0.26
	b_T (kJ/mol)	99.1	5.1	9.5
	R^2	0.95	0.90	0.82

In comparison with adsorbents that have similar iron oxide modification such as IOCS and IOCS-2, the modifications made in Fe[a]-VMO and Zr[a]-VMO improved the As(V) adsorption capacity considerably. For example, IOCS and IOCS-2 had As(V) adsorption capacity of 0.018 mg/g and 0.008 mg/g at initial As(V) concentration of 0.325 mg/L and 0.1 mg/L, respectively (Mohan and Pittman Jr 2007; Thirunavukkarasu et al. 2001). Nevertheless, in comparison with other natural manganese ores, As(V) adsorption capacity of unmodified VMO is lower. For instance, manganese oxide (MO1) from France had a capacity of 0.172 mg/g at an initial As(V) concentration (C_0) < 1 mg As(V)/L (Mohan and Pittman Jr 2007; Ouvrard et al. 2002).

3.4.2 Adsorption kinetics

The adsorption kinetics of original and modified VMO were conducted at pH 7.0 ± 0.2 with the same initial As(V) concentration of 0.5 mg/L. This kinetics study can help to understand the mechanism of adsorption of As(V) onto VMO and its modified forms (Puttamat and Pavarajarn 2016). The experimental results show that As(V) was adsorbed rapidly within the first 30 min when there were enough adsorption sites for As(V) adsorption (Fig. 8). Then, the process slowed down because of the gradual saturation of adsorption sites.

Pseudo-first order (PFO), pseudo-second order (PSO) and Elovich models were applied to investigate the adsorption kinetics of As(V). The values of model parameters and correlation coefficients obtained from the plots are presented in Table 5. According to the values of R^2, the PFO and PSO models fitted the data comparatively better than the Elovich model.

Finally, the Elovich model was used to describe the kinetics adsorption data. This model also explained the data well, though the R^2 values were slightly lower than those for PFO and PSO models. The good fit of the model to data is consistent with the chemisorption mechanism (Adeogun and Babu 2015; Firdaous et al. 2017; Önal 2006) for arsenic shown by zeta potential data. The α value was much higher for Fe[a]-VMO and Zr[b]-VMO than for VMO (Table 5) indicating that the initial rate of adsorption was higher for the modified VMOs. This could be due to the increased affinity of Fe and Zr in VMO to arsenic. However, the β value which is a reciprocal of the number of sites available for adsorption (Adeogun and Babu 2015), was higher for VMO, indicating that the number of sites available for adsorption was lower for VMO with higher activation energy for chemisorption on VMO (Firdaous et al. 2017).
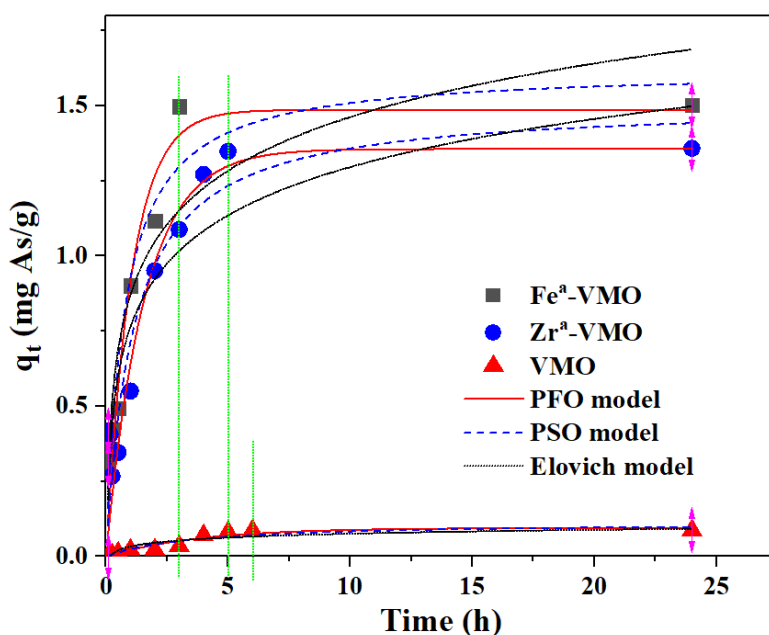

Fig. 8. Adsorption kinetics models fit to the data on As(V) adsorption on modified and un-modified VMO

Table 5. Parameter values for batch adsorption kinetics

Model	Parameter	Adsorbent		
		VMO	Fe[a]-VMO	Zr[a]-VMO
	q_{exp} (mg As/g)	0.09	1.50	1.36
Pseudo-first order	q_e (mg As/g)	0.10	1.49	1.36
	k_1 (h^{-1})	0.26	0.96	0.63
	R^2	0.92	0.94	0.88
Pseudo-second order	q_e (mg As/g)	0.11	1.62	1.51
	k_2 (g/mg.h)	2.42	0.82	0.59
	R^2	0.89	0.94	0.88
Elovich	α (mg/g.min)	0.002	0.125	0.105
	β (g/mg)	53.8	3.88	4.32
	R^2	0.82	0.88	0.83

3.5 Influence of pH on As(V) adsorption

The As(V) adsorption depends on the pH of the solution because pH affects the protonation/deprotonation of the adsorbate, the surface charge of the adsorbents, the degree of ionisation of the surface groups and the nature of the adsorbing ions (Puttamat and Pavarajarn 2016; Worch 2012). Fig. 9 illustrates a significant decline in the As(V) adsorption efficiency (E%) when the pH rose from 3 to 10 for all three adsorbents. This phenomenon is due to the decrease in positive zeta potential or increase in negative zeta potential as pH increased from 3 to 10 (Fig. 4). The increase in surface negative charge repels the negatively charged As(V) anions. Also, the negative charge on the As(V) anions increases as pH increases producing unfavourable conditions for adsorption. Another reason for the decreased adsorption at high pH is that at high pH the concentration of OH$^-$ anions increases and it competes with As(V) for adsorption. Others have also reported a reduction in As(V) adsorption when pH increases for other adsorbents (Camacho et al. 2011; Wu et al. 2017).
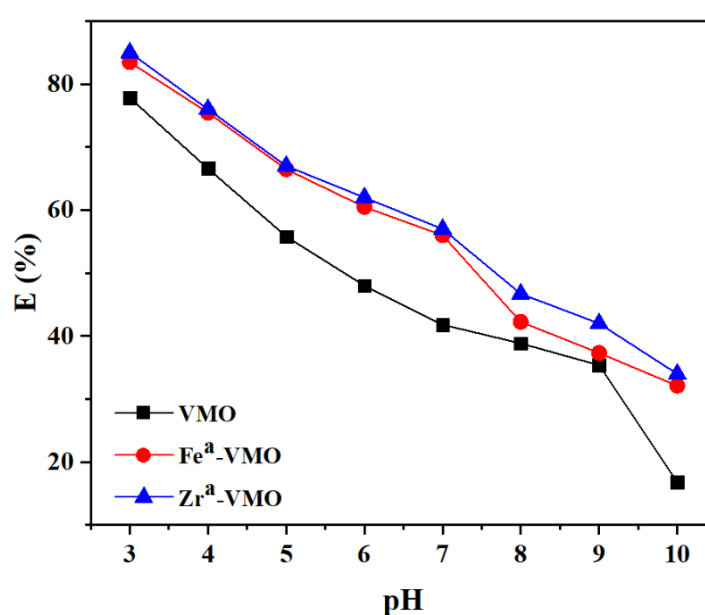

Fig. 9. Influence of pH on As(V) removal efficiency of VMO (3.0 g/L), Fe[a]-VMO (0.3 g/L) and Zr[a]-VMO (0.3 g/L)

3.6 Effect of co-existing anions on As(V) adsorption

In nature, many ions are present along with As in water and some of them can impact the As adsorption ability of an adsorbent. In this study, the prominent anions present in water, PO_4^{3-}, SO_4^{2-}, SiO_3^{2-} and CO_3^{2-}, were selected for analysis at different concentrations (0.1, 1, 5, 10, 20 mg/L) to evaluate their effects on As(V) adsorption.

As can be seen from Fig. 10, at the lowest concentration of 0.1 mg/L, all anions exerted only minor influence on As(V) adsorption efficiency. When their concentration increased to more than 5 mg/L, the effect of PO_4^{3-} and SiO_3^{2-} was significantly higher than that of CO_3^{2-} and SO_4^{2-}. This observation is consistent with previous studies, which reported silicate and phosphate competing with As for adsorption (Ciardelli et al. 2008). The presence of 20 mg/L of PO_4^{3-} in solution reduced the As removal efficiency of the three adsorbents by about 60 - 70%. The effect of SiO_3^{2-} followed that of PO_4^{3-} with reductions of 47%, 34% and 26% As(V) removal efficiency of VMO, Fe[a]-VMO and Zr[a]-VMO, respectively. This is because these oxyanions were strongly adsorbed by $M(OH)_n$, where M is a metal ion such as Fe^{3+}, Mn^{4+}, Zr^{4+}, etc. The oxyanion, CO_3^{2-} and SO_4^{2-}, did not have much effect on arsenic removal. Consequently, the sequence of competitive anions hindering the sorption of As(V) is $PO_4^{3-}>$ $SiO_3^{2-} > CO_3^{2-} > SO_4^{2-}$. Gu et al. (2005) and Ren et al. (2011) also reported that PO_4^{3-} and SiO_3^{2-} reduced As(V) adsorption on Fe modified GAC more than CO_3^{2-} and SO_4^{2-}.
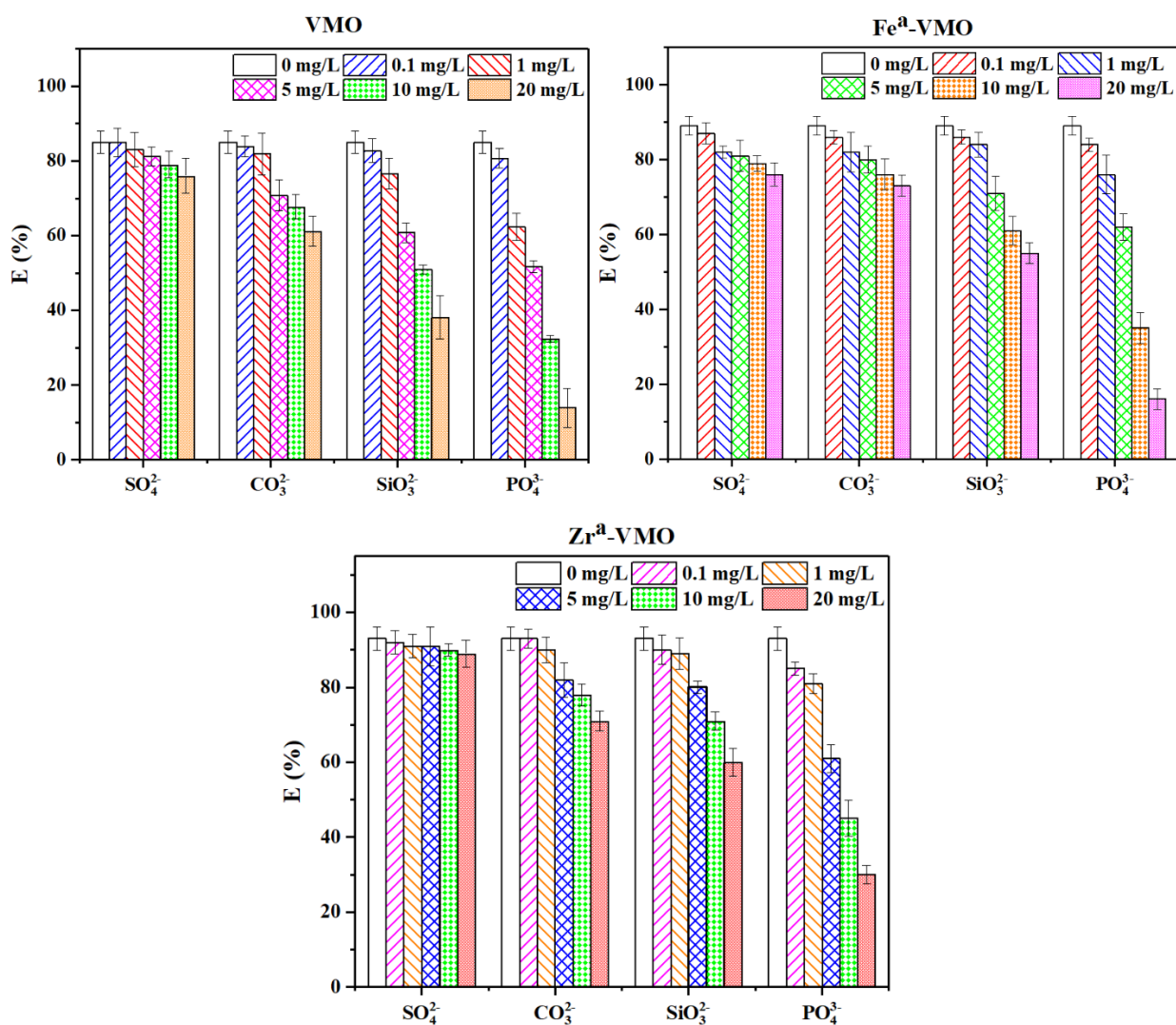

Fig. 10. Effects of co-existing anions on As(V) removal at fixed initial As(V) concentration of 0.5 mg/L

4. Conclusions

As a low-cost commercial adsorbent, VMO was employed to remove arsenic from groundwater in many treatment systems in Vietnam. However, the As(V) removal capacity of pure VMO is not sufficiently high.

Mixing VMO with ferric nitrate or zirconium nitrate and sodium hydroxide and heating at 110 ^{0}C and 550 ^{0}C emerged as the best out of four methods of modification of VMO to improve As(V) removal. The Langmuir adsorption capacities of the modified materials, Fe[a]-VMO and Zr[a]-VMO at pH 7.0 were 2.19 and 1.94 mg As/g, respectively, which are approximately 20 times higher than that of the unmodified VMO. Zeta potential data showed that the greater As(V) adsorption by the modified adsorbents could be due to inner-sphere complexation of As(V) with Fe and Zr oxide/hydroxides coatings on VMO, as well as outer-sphere complexation of As(V) with the Fe/Mn coatings which provided increased positive charges for electrostatic adsorption of negatively charged As species. Langmuir, Freundlich and Temkin models were applied successfully to describe the equilibrium adsorption of As(V) onto the original and modified VMO. The adsorption kinetics data also fitted well to the three models, pseudo-first order, pseudo-second order and Elovich models. The As(V) removal efficiency increased by up to 50 - 60% when pH progressively declined from 10 to 3. The PO_4^{3-} and SiO_3^{2-} co-ions had a strong competitive effect on As(V) removal efficiency. In contrast, the ions, CO_3^{2-} and SO_4^{2-} had little influence on As(V) removal.

References

Adeogun AI, Babu RB (2015) One-step synthesized calcium phosphate-based material for the removal of alizarin S dye from aqueous solutions: isothermal, kinetics, and thermodynamics studies. Appl Nanosci 1-13

Ahmed MF (2001) An overview of arsenic removal technologies in Bangladesh and India. In: Proceedings of BUET-UNU international workshop on technologies for arsenic removal from drinking water, Dhaka, Bangladesh 5-7

Altundoğan HS, Altundoğan S, Tümen F, Bildik M (2002) Arsenic adsorption from aqueous solutions by activated red mud. Waste Manage 22:357-363

Amini M, Abbaspour KC, Berg M, Winkel L, Hug SJ, Hoehn E, Yang H, Johnson (2008) Statistical modeling of global geogenic arsenic contamination in groundwater. Environ Sci Tech 42:3669-3675

Asere TG, Stevens CV, Du Laing G (2019) Use of (modified) natural adsorbents for arsenic remediation: A review. Sci Total Environ 676:706-720

Berg, M., C. Stengel, P. T. K. Trang, P. H. Viet, M. L. Sampson, M. Leng, S. Samreth and D. Fredericks (2007) Magnitude of arsenic pollution in the Mekong and Red River Deltas-Cambodia and Vietnam. Sci Total Environ 372:413-425

Berg M, Tran HC, Nguyen TC, Pham HV, Schertenleib R, Giger W (2001) Arsenic contamination of groundwater and drinking water in Vietnam: a human health threat. Environ Sci Tech 35:2621-2626

Buschmann J, Berg M, Stengel C, Sampson ML (2007) Arsenic and manganese contamination of drinking water resources in Cambodia: coincidence of risk areas with low relief topography. Environ Sci Tech 41:2146-2152

Camacho LM, Parra RR, Deng S (2011) Arsenic removal from groundwater by MnO$_2$-modified natural clinoptilolite zeolite: Effects of pH and initial feed concentration. J Hazard Mater 189:286-293

Chakraborti D, Rahman MM, Paul K, Chowdhury UK, Sengupta MK, Lodh D, Chanda CR, Saha KC, Mukherjee SC (2002) Arsenic calamity in the Indian subcontinent: what lessons have been learned? Talanta 58:3-22

Chakravarty S, Dureja V, Bhattacharyya G, Maity S, Bhattacharjee S (2002) Removal of arsenic from groundwater using low cost ferruginous manganese ore. Water Research 36:625-632

Chiban M, Zerbet M, Carja G, Sinan F (2012) Application of low-cost adsorbents for arsenic removal: A review Journal of Environmental Chemistry and Ecotoxicology 4:91-102

Ciardelli MC, Xu H, Sahai N (2008) Role of Fe (II), phosphate, silicate, sulfate, and carbonate in arsenic uptake by coprecipitation in synthetic and natural groundwater Water Res 42:615-624

Dada A, Olalekan A, Olatunya A, Dada O (2012) Langmuir, Freundlich, Temkin and Dubinin–Radushkevich isotherms studies of equilibrium sorption of Zn^{2+} unto phosphoric acid modified rice husk. IOSR J Appl Chem 3:38-45

Delva L, Verberckmoes A, Cardon L, Ragaert K (2013) The use of rubber as a compatibilizer for injection moulding of recycled post-consumer mixed polyolefines. In: 2nd International Conference WASTES: Solutions, Treatments and Opportunities. CVR, Braga, Portugal

Erhayem M, Al-Tohami F, Mohamed R, Ahmida K (2015) Isotherm, kinetic and thermodynamic studies for the sorption of mercury (II) onto activated carbon from Rosmarinus officinalis leaves. American J Ana Chem 6:1

Firdaous L, Fertin B, Khelissa O, Dhainaut M, Nedjar N, Chataigné G, Ouhoud L, Lutin F, Dhulster P (2017) Adsorptive removal of polyphenols from an alfalfa white proteins concentrate: Adsorbent screening, adsorption kinetics and equilibrium study. Sep Purif Tech 178:29-39

Gu Z, Fang J, Deng B (2005) Preparation and evaluation of GAC-based iron-containing adsorbents for arsenic removal. Environ Sci Tech 39:3833-3843

Hang C, Li Q, Gao S, Shang JK (2011) As (III) and As (V) adsorption by hydrous zirconium oxide nanoparticles synthesized by a hydrothermal process followed with heat treatment. Ind Eng Chem Res 51:353-361

Järup L (2003) Hazards of heavy metal contamination. Br Méd Bull 68:167-182

Jia Y, Xu L, Wang X, Demopoulos GP (2007) Infrared spectroscopic and X-ray diffraction characterization of the nature of adsorbed arsenate on ferrihydrite. Geochim Cosmochim Ac 71:1643-1654

Kabir F, Chowdhury S (2017) Arsenic removal methods for drinking water in the developing countries: technological developments and research needs. Environ Sci Poll Res 24:24102-24120

Kalaruban M, Loganathan P, Shim W, Kandasamy J, Naidu G, Nguyen TV, Vigneswaran S (2016) Removing nitrate from water using iron-modified Dowex 21K XLT ion exchange resin: Batch and fluidised-bed adsorption studies. Sep Purif Tech 158:62-70

Khan TA, Chaudhry SA, Ali I (2013) Thermodynamic and kinetic studies of As (V) removal from water by zirconium oxide-coated marine sand. Environ Sci Poll Res 20:5425-5440

Loganathan P, Vigneswaran S, Kandasamy J, Bolan NS (2014) Removal and recovery of phosphate from water using sorption. Crit Rev Environ Sci Tech 44:847-907

Maiti A, Basu JK, De S (2010) Development of a treated laterite for arsenic adsorption: effects of treatment parameters. Ind Eng Chem Res 49:4873-4886

Mamindy-Pajany Y, Hurel C, Marmier N, Roméo M (2011) Arsenic (V) adsorption from aqueous solution onto goethite, hematite, magnetite and zero-valent iron: effects of pH, concentration and reversibility. Desalination 281:93-99

Markovski JS, Marković DD, Đokić VR, Mitrić M, Ristić MĐ, Onjia AE, Marinković AD (2014) Arsenate adsorption on waste eggshell modified by goethite, α-MnO2 and goethite/α-MnO$_2$. Chem Eng J 237:430-442

Mohan D, Pittman Jr CU (2007) Arsenic removal from water/wastewater using adsorbents-a critical review. J Hazard Mater 142:1-53

Mondal P, Balomajumder C, Mohanty B (2007) A laboratory study for the treatment of arsenic, iron, and manganese bearing ground water using Fe3+ impregnated activated carbon: Effects of shaking time, pH and temperature. J Hazard Mater 144:420-426

Myneni SC, Traina SJ, Waychunas GA, Logan TJ (1998) Vibrational spectroscopy of functional group chemistry and arsenate coordination in ettringite. Geochim Cosmochim Ac 62:3499-3514

Nur T, Johir M, Loganathan P, Nguyen T, Vigneswaran S, Kandasamy J (2014) Phosphate removal from water using an iron oxide impregnated strong base anion exchange resin. J Ind Eng Chem 20:1301-1307

Oladoja N, Helmreich B (2014) Batch defluoridation appraisal of aluminium oxide infused diatomaceous earth. Chem Eng J 258:51-61

Önal Y (2006) Kinetics of adsorption of dyes from aqueous solution using activated carbon prepared from waste apricot. J Hazard Mater 137:1719-1728

Ouvrard S, Simonnot M-O, Sardin M (2002) Reactive behavior of natural manganese oxides toward the adsorption of phosphate and arsenate. Ind Eng Chem Res 41:2785-2791

Petit T, Puskar L (2018) FTIR spectroscopy of nanodiamonds: Methods and interpretation. Diam Relat Mater

Pokhrel D, Viraraghavan T (2008) Arsenic removal from an aqueous solution by modified A. niger biomass: batch kinetic and isotherm studies. J Hazard Mater 150:818-825

Polya D, Gault A, Diebe N, Feldman P, Rosenboom J, Gilligan E, Fredericks D, Milton AH, Sampson M, Rowland HAL (2005) Arsenic hazard in shallow Cambodian groundwaters. Mineral Mag 69:807-823

Puttamat S, Pavarajarn V (2016) Adsorption study for removal of Mn (II) ion in aqueous solution by hydrated ferric (III) oxides. Inter J Chem Eng Appl 7:239-243

Qiu H, Lv L, Pan B-c, Zhang Q-j, Zhang W-m, Zhang Q-x (2009) Critical review in adsorption kinetic models. J Zhejiang University-Sci A 10:716-724

Ren Z, Zhang G, Paul Chen J (2011) Adsorptive removal of arsenic from water by an iron-zirconium binary oxide adsorbent. J Colloid Interf Sci 358:230-237

Shahmohammadi-Kalalagh S (2011) Isotherm and kinetic studies on adsorption of Pb, Zn and Cu by kaolinite. Casp J Environ Sci 9:243-255

Smedley PL, Kinniburgh D (2002) A review of the source, behaviour and distribution of arsenic in natural waters. Appl Geochem 17:517-568

Sogaard E (2014) Chemistry of advanced environmental purification processes of water: Fundamentals and applications. Amst: Elsevier.

Thirunavukkarasu O, Viraraghavan T, Subramanian K (2001) Removal of arsenic in drinking water by iron oxide-coated sand and ferrihydrite-batch studies. Water Qual Res J 36:55-70

Thirunavukkarasu O, Viraraghavan T, Subramanian K (2003) Arsenic removal from drinking water using iron oxide-coated sand. Water Air Soil Poll 142:95-111

Tomić ZP, Antić-Mladenović SB, Babić BM, Poharc-Logar VA, Đorđević AR, Cupać SB (2011) Modification of smectite structure by sulfuric acid and characteristics of the modified smectite. J Agricul Sci 56:25-35

Worch E (2012) Adsorption technology in water treatment: fundamentals, processes, and modeling. Walter de Gruyter

Wu C, Tu J, Liu W, Zhang J, Chu S, Lu G, Lin Z, Dang Z (2017) The double influence mechanism of pH on arsenic removal by nano zero valent iron: electrostatic interactions and the corrosion of Fe 0. Environ Sci: Nano 4:1544-1552

Wu F-C, Tseng R-L, Juang R-S (2009) Characteristics of Elovich equation used for the analysis of adsorption kinetics in dye-chitosan systems. Chem Eng J 150:366-373

Zhang G, Liu H, Liu R, Qu J (2009) Adsorption behavior and mechanism of arsenate at Fe-Mn binary oxide/water interface. J Hazard Mater 168:820-825

Zhou Z, Liu Y-g, Liu S-b, Liu H-y, Zeng G-m, Tan X-f, Yang C-p, Ding Y, Yan Z-l, Cai X-x (2017) Sorption performance and mechanisms of arsenic(V) removal by magnetic gelatin-modified biochar. Chem Eng J 314:223-231